



HAL
open science

Fe/Mg O interface engineering for high-output-voltage device applications

Coriolan Tiusan, M. Sicot, Michel Hehn, C. Belouard, S. Andrieu, F. Montaigne, Alain Schuhl

► **To cite this version:**

Coriolan Tiusan, M. Sicot, Michel Hehn, C. Belouard, S. Andrieu, et al.. Fe/Mg O interface engineering for high-output-voltage device applications. Applied Physics Letters, 2006, 88 (6), pp.062512. 10.1063/1.2172717 . hal-04370098

HAL Id: hal-04370098

<https://hal.science/hal-04370098>

Submitted on 1 Aug 2024

HAL is a multi-disciplinary open access archive for the deposit and dissemination of scientific research documents, whether they are published or not. The documents may come from teaching and research institutions in France or abroad, or from public or private research centers.

L'archive ouverte pluridisciplinaire **HAL**, est destinée au dépôt et à la diffusion de documents scientifiques de niveau recherche, publiés ou non, émanant des établissements d'enseignement et de recherche français ou étrangers, des laboratoires publics ou privés.

RESEARCH ARTICLE | FEBRUARY 09 2006

Fe / Mg O interface engineering for high-output-voltage device applications

C. Tiusan; M. Sicot; M. Hehn; C. Belouard; S. Andrieu; F. Montaigne; A. Schuhl



Appl. Phys. Lett. 88, 062512 (2006)
<https://doi.org/10.1063/1.2172717>



Nanotechnology & Materials Science


Optics & Photonics

Impedance Analysis

Scanning Probe Microscopy


Sensors

Failure Analysis & Semiconductors



Unlock the Full Spectrum.
From DC to 8.5 GHz.
Your Application. Measured.

[Find out more](#)



Fe/MgO interface engineering for high-output-voltage device applications

C. Tiusan, M. Sicot, M. Hehn, C. Belouard, S. Andrieu, F. Montaigne, and A. Schuhl
Laboratoire de Physique des Matériaux, UMR CNRS 7556, B.P. 239, 54506 Vandœuvre lès Nancy Cedex, France

(Received 31 May 2005; accepted 22 December 2005; published online 9 February 2006)

The magnetotransport characteristics of Fe/MgO/Fe epitaxial tunnel junctions are reported. For clean Fe/MgO interfaces, a tunnel magnetoresistance of 150% is measured. However, the magnetoresistance decreases rapidly with the applied voltage. Consequently, the main parameter to optimize for device application, namely the output voltage, remains relatively low. This limitation has been solved by interface engineering through the insertion of carbon impurities at the Fe/MgO interface. Although the tunnel magnetoresistance amplitude is slightly reduced, its variation versus the applied voltage becomes strongly asymmetric with large magnetoresistance maintained up to 1.5 V. This determines a large increase of the tunnel junction output voltage. © 2006 American Institute of Physics. [DOI: 10.1063/1.2172717]

The already wide application prospects¹ of devices based on magnetic tunnel junction (MTJ), have been recently boosted by the observation of large tunnel magnetoresistance (TMR) in MgO crystalline oxide based tunnel junction.²⁻⁴ Although the measured value, above 200%, is already 3 times larger than in standard amorphous alumina barriers, the *ab initio* calculations⁵⁻⁷ performed on epitaxial MTJ systems predict even higher TMR. However, it needs to increase the barrier thickness. Consequently the resistance of the MTJ becomes too high for most of the applications. Recently, we have already proven the direct impact of the electronic structure on spin polarized transport in Fe/MgO/Fe epitaxial magnetic tunnel junctions.⁸ In this letter, we show that interface engineering of this electronic structure, through the insertion of carbon impurities at the Fe/MgO interface, increases radically the output voltage which is the main parameter to optimize for device applications.

The MTJ multilayer stacks subjected to our studies have been elaborated by molecular beam epitaxy (MBE), in a chamber with a base pressure of 5×10^{-11} Torr. Two set of samples have been grown on (100) MgO substrates, previously annealed at 600 °C for 20 min. For the sample type A, a 50-nm-thick bottom Fe layer was deposited at room temperature directly on the MgO substrate. For the sample type B, a 10 nm thick seed MgO underlayer was grown at 450 °C on the substrate, before the deposition of the 50-nm-thick Fe layer. This MgO underlayer acts as an antidiffusion barrier. It traps the residual carbon impurities from the substrate surface and prevents their diffusion within the layers during subsequent annealing stages.⁹ Indeed, to improve its surface quality, the bottom Fe layer was annealed at 450 °C for 20 min. The surface rms roughness after annealing, estimated from atomic force microscopy analysis, was about 0.1 nm. However, the Fe top surfaces, postannealing, are not equivalent for samples type A and B, as highlighted in Fig. 1 containing reflecting high energy electron diffraction (RHEED) patterns. For both sets of samples the RHEED patterns along the [110] direction (not shown here) are identical and they are characteristic of the bcc Fe(100) structure. However, along the [100] direction, the RHEED analysis of sample type A emphasizes a $c(2 \times 2)$ reconstruction-related additional pattern, not present for sample B. A complete

RHEED analysis, concludes that in samples type A the Fe surface postannealing presents a $c(2 \times 2)$ superstructure. In agreement with results of previous Auger electron spectroscopy and quantitative low-energy electron diffraction (LEED) studies,¹⁰ we associate this reconstruction to the segregation of C at the Fe(001) surface. Using Auger analysis we checked the chemical nature the surface and we confirmed that for sample type A, a carbon monolayer was segregated during the Fe annealing. Where does the C come from? We observed that the annealing stage of the MgO substrate at 600 °C does not desorb all the C atoms from the surface. In the case when the antidiffusion 10 nm MgO thick underlayer is not inserted (sample type A), the residual C atoms diffuse and segregate to the Fe top surface and provide the surface reconstruction during the bottom Fe layer annealing. However, Auger spectroscopy analysis revealed no C contamination after the deposition of the 3 nm thick 3 nm MgO barrier (the C remains trapped at the bottom Fe/MgO interface). On the other hand, in the samples type B, the trapping underlayer of MgO provides a C free Fe top surface, postannealing. As it will be shown later, the chemical structure of the Fe surface has a strong impact on the magnetotransport characteristics of the junctions, mainly reflected

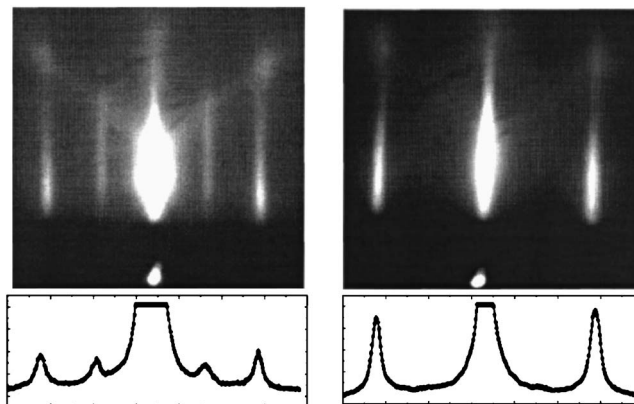


FIG. 1. RHEED pattern measured along the [100] direction after the growth of the 50 nm thick Fe bottom layer for sample B. A profile highlights 3 peaks; right: RHEED pattern measured along the [100] direction after the growth of the Fe bottom layer and adjunction of C for sample A. A profile highlights 2 additional peaks characteristic of the 2×2 reconstruction.

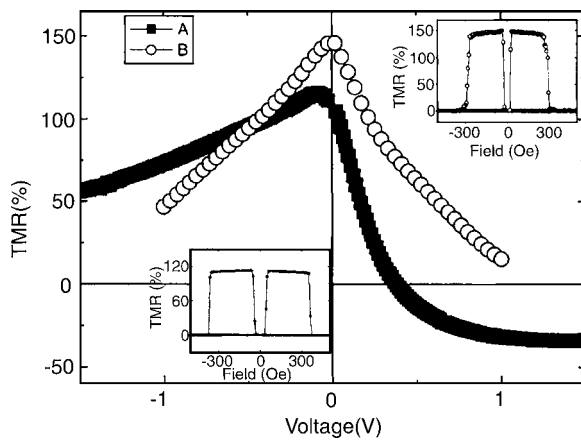


FIG. 2. Magnetoresistance as a function of applied voltage measured on a Fe/MgO/Fe tunnel junction (\circ) and on a Fe/C/MgO/Fe tunnel junction (\bullet). The right top inset shows a characteristic resistance versus applied field measured on a Fe/MgO/Fe tunnel junction at 10 mV (\circ) and the left bottom inset shows a characteristic resistance versus applied field measured on a Fe/C/MgO/Fe tunnel junction at 10 mV (\bullet).

by the TMR versus applied voltage behavior.

On the top of the bottom Fe layer, a 3.0 nm thick MgO insulating layer was epitaxially grown by means of an electron gun. A two-dimensional layer-by-layer growth was observed up to 5 monolayers by means of RHEED intensity oscillations.¹¹ A second magnetic 10-nm-thick Fe layer was epitaxially grown on the top of the insulating MgO barrier at 100 °C. For sample type B, this layer was subsequently annealed for flattening at 380° for 10 min, whereas for the sample type A the annealing was not done in order to avoid modifications of the bottom C related $c(2 \times 2)$ reconstructed Fe/MgO interface. This top Fe layer is magnetically hardened by a 20 nm Co layer, deposited on top. The stack was capped with a Pd(10 nm)/Au(10 nm) protecting bilayer.

After the MBE growth of the multilayer stack, the MTJ structures were patterned by UV lithography and Ar ion etching, step-by-step controlled *in situ* by Auger spectroscopy.¹²

Let us consider first the TMR(V) characteristics, measured on sample B (Fig. 2, \circ). As predicted theoretically,⁵⁻⁷ for large MgO thickness in the asymptotic regime, the tunneling is found to be dominated by a majority spd -like character state Δ_1 in the parallel (P) configuration.¹³ The propagation of this state in the antiparallel (AP) configuration is “prohibited,” which corresponds to a strongly reduced conductivity. In agreement with this framework, we measure a large TMR signal of 150% at room temperature. However, the TMR value decreases rapidly with applied voltage. The voltage for which the tunnel magnetoresistance is divided by a factor of 2, $V_{1/2}$, remains here below 0.5 V. The origin of this rapid decay of the TMR with voltage in standard Fe/MgO/Fe is addressed more in detail elsewhere.¹⁴

On the other hand, the TMR(V) characteristic measured on sample A, with carbon impurities at the bottom Fe/MgO interface, appears strongly asymmetric with a maximum of TMR of 126% at room temperature. One can immediately remark the sign reversal of the TMR in positive voltage. In our previous work,⁸ this was associated to the contribution to the tunneling of the interfacial resonance of Fe in Fe/MgO/Fe MTJ with thinner MgO barriers. However, here—at large MgO thickness—the contribution to the tunneling of the interfacial resonance (with d_{z^2} orbital characte,

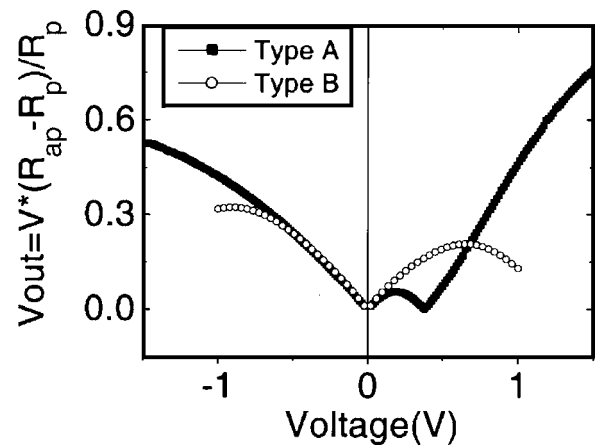


FIG. 3. Output voltage versus applied voltage measured on a Fe/MgO/Fe tunnel junction (\circ) and on a Fe/C/MgO/Fe tunnel junction (\bullet).

should be less significant. This is exactly what we observe in samples type B with carbon free interfaces. However, when carbon impurities are inserted at the Fe/MgO bottom interface, the bonding between C and Fe seems to enhance the contribution to the tunneling of the interfacial resonance of Fe (located in a d -like orbital). The exact mechanism responsible on this behavior requires further theoretical investigation.

For positive biasing of the bottom electrode, the electrons, extracted from the top Fe(001) electrode by tunneling across the barrier, “scan” in energy the bottom “flat” Fe(001) electronic structure. Then, when the energy of the collected electrons “matches” the energy of the interface resonant state, a strong enhancement of the antiparallel conductivity with respect to the parallel one occurs, via the enhancement of the wave function matching at the interface. This explains the sign reversal of the TMR (Fig. 2, \bullet) when the antiparallel conductance overcomes the parallel one, above 0.3 eV. Moreover, the structural quality of the top MgO/Fe interface is reduced with respect to the atomically flat bottom one. Indeed, the bottom Fe was annealed at 450° whereas the top Fe electrode in junctions type A was not. The RHEED patterns and also the atomic force microscopy experiments validate a significantly higher roughness of the top Fe electrode in sample type A. One can assume that the interfacial resonance is destroyed by roughness for this electrode, and also that the density of states of the rough electrode presents no sharp features. Then, for negative voltage, when the electrons tunnel towards the rough top electrode positively biased, we observe a very small variation of the magnetoresistance versus V ($V_{1/2} > 1.5$ V). Moreover, the extremely small decay of the TMR with the applied voltage implicates that an additional mechanism competes with all the mechanisms responsible for the zero bias anomaly, observed in sample type B, where a significant decay of the TMR with bias has been measured.¹⁴ It is related to an additional electronic-structure-related filtering effect for tunneling electrons, activated by the chemical bonding via the interfacial carbon. Moreover, the roughness-induced annihilation of the surface state reduces the probability of resonant spin-flip assisted tunneling mechanism and prevents the voltage decay of the TMR.

For device application, the key parameter is the magnitude of the output signal modulation, namely the output voltage defined as $V_{out} = V(R_{ap} - R_p)/R_{ap}$, where V is the applied voltage, R_{ap} and R_p are the junction resistances measured

with antiparallel and parallel alignment of MTJ ferromagnetic layers. From the TMR ratio as a function of the bias voltage, the output voltage for device applications is plotted against bias voltage in Fig. 3 for sample A and B. For sample type B, which provides the highest TMR amplitude, the V_{out} in positive bias voltages can exceed 300 mV. This value is already almost two times larger than the values measured for conventional MTJs with an AlO barriers. Recently, the state of the art for V_{out} has been reported to be of 500 mV.² However, as shown in Fig. 3, we illustrate here that this V_{out} can be further increased by interface engineering, namely the insertion of C at the Fe/MgO interface. Therefore, we obtain a V_{out} that can reach 0.8 V, which represents a new state of the art in this field area.

The conventional use of high values for both TMR and $V_{1/2}$ to provide large V_{out} is replaced here by a new mechanism. The specific filtering effect related to C contaminated Fe/MgO interfacial electronic structure,¹⁴ induces a change of the tunnel magnetoresistance sign. The inverse TMR, remains quasi constant at bias voltages beyond 1 V, reaching values above -40% . This, combined with the small tunnel resistance of the junction biased beyond 1 V, drives to large values of the junction output voltage. One the other hand, even in the branch with positive TMR, the voltage variation of the magnetoresistive effect is significantly reduced in junctions with C at the bottom interface. These results, illustrate how the interface engineering in Fe/MgO/Fe MTJs may be used as a key technology in engineering the properties of novel spintronic devices.

The authors acknowledge J. Faure-Vincent and D. Stoeffler for useful discussions, and D. Ligiardi and M. Alnot for technical support.

- ¹S. A. Wolf, *J. Supercond.* **13**, 195 (2000).
- ²S. Yuasa, T. Nagahama, A. Fukushima, Y. Suzuki, and K. Ando, *Nano Lett.* **3**, 868 (2004).
- ³S. S. P. Parkin, C. Kaiser, A. Panchula, P. M. Rice, B. Hughes, M. Samant, and S.-H. Yang, *Nano Lett.* **3**, 862 (2004).
- ⁴D. D. Djayaprawira, K. Tsunekawa, M. Nagai, H. Maehara, S. Yamagata, N. Watanabe, S. Yuasa, Y. Suzuki, and K. Ando, *Appl. Phys. Lett.* **86**, 092502 (2005).
- ⁵J. M. MacLaren, X.-G. Zhang, W. H. Buttler, and X. Wang, *Phys. Rev. B* **59**, 5470 (1999).
- ⁶W. H. Butler, X.-G. Zhang, T. C. Schulthess, and J. M. MacLaren, *Phys. Rev. B* **63**, 054416 (2001).
- ⁷J. Mathon and A. Umerski, *Phys. Rev. B* **63**, 220403 (2001).
- ⁸C. Tiusan, J. Faure-Vincent, C. Bellouard, M. Hehn, E. Jouguelet, and A. Schuhl, *Phys. Rev. Lett.* **93**, 106602 (2004).
- ⁹Residual carbon persists on the MgO substrate surface even after the annealing at 600°. Without the additional trap, these impurities diffuse across the Fe buffer layer during subsequent annealing stages.
- ¹⁰V. Blum, A. Schmidt, W. Meier, L. Hammer, and K. Heinz, *J. Phys.: Condens. Matter* **15**, 3517 (2003).
- ¹¹E. Popova, J. Faure-Vincent, C. Tiusan, C. Bellouard, H. Fischer, M. Hehn, F. Montaigne, M. Alnot, S. Andrieu, A. Schuhl, E. Snoeck, and V. da Costa, *Appl. Phys. Lett.* **81**, 1035 (2002).
- ¹²J. Faure-Vincent, C. Tiusan, E. Jouguelet, F. Canet, M. Sajjeddine, C. Bellouard, E. Popova, M. Hehn, F. Montaigne, and A. Schuhl, *Appl. Phys. Lett.* **82**, 4507 (2003).
- ¹³X.-G. Zhang, W. H. Butler, and A. Bandyopadhyay, *Phys. Rev. B* **68**, 092402 (2003).
- ¹⁴C. Tiusan, M. Sicot, J. Faure-Vincent, M. Hehn, C. Bellouard, F. Montaigne, S. Andrieu, and A. Schuhl, *J. Phys.: Condens. Matter* **18**, 941 (2005). The voltage variation of the TMR is related to the interfacial resonant inelastic tunneling mechanisms, determined by the minority surface state of Fe(001).